buildings

MDPI

Article

Performance of Asphalt Mastic and Asphalt Mixture with Harmless Municipal Solid Waste Incineration Fly Ash

Erxin Li [1], Xiangyu Zhang [1,*], Liyong Wang [2], Rui Wang [3], Wei Zhang [3], Chengqin Chen [3] and Wengang Zhang [4,*]

[1] The Highway Development Center of Gansu Province, Lanzhou 730030, China
[2] China Highway Engineering Consulting Corporation, Beijing 100089, China
[3] School of Civil Engineering, Northwest Minzu University, Lanzhou 730030, China
[4] School of Civil and Architectural Engineering, Shandong University of Technology, Zibo 255049, China
* Correspondence: xaingyu1984@126.com (X.Z.); ziwuzizwg@sdut.edu.cn (W.Z.)

Abstract: In this paper, harmless municipal solid waste incineration fly ash (H-MSWIFA) was used to replace part of the mineral powder in asphalt mastic prepared with different ratios of filler to asphalt (F/A). Cone penetration (CPT), rotational viscosity, low-temperature bending, and full section fracture energy(FSFET) tests on the prepared H-MSWIFA asphalt mastic were carried out to evaluate the viscosity at room temperature, viscosity at high temperature, tensile property at low temperature, and crack resistance at room temperature of the asphalt mastic with different F/A and different H-MSWIFA content. An asphalt concrete mixture with a nominal maximum particle size of 13 mm (AC-13) with different F/A and H-MSWIFA replacement ratios was prepared. The effects of F/A and H-MSWIFA content on the high-temperature stability, water stability, and low-temperature cracking resistance of the asphalt mixture were studied. The results showed that the shear strength and viscosity of the asphalt mastic increased after H-MSWIFA replaced part of the mineral powder; and the greater the F/A, the greater the shear strength and viscosity of the asphalt mastic. H-MSWIFA can greatly improve the viscosity of asphalt mastic at high temperatures, and with the increase in H-MSWIFA content, the improvement effect becomes more obvious. The high-temperature stability of the asphalt mixture is not related to H-MSWIFA content but mainly depends on the F/A. Both the F/A and the H-MSWIFA replacement ratio can significantly affect the water stability of the asphalt mixture, specifically, the water stability reaches the best value when the F/A is around 1.0, and the addition of H-MSWIFA harms water stability. Both the F/A and the H-MSWIFA replacement ratio can significantly affect the low-temperature cracking resistance of the asphalt mixture. The higher the F/A, the worse the low-temperature crack resistance. At the same time, the addition of H-MSWIFA harms low-temperature cracking resistance. From the point of view of water stability and low-temperature crack resistance of the asphalt mixture, the H-MSWIFA replacement ratio should not be too high.

Keywords: H-MSWIFA; F/A; H-MSWIFA content; asphalt mastic; asphalt mixture

check for updates

Citation: Li, E.; Zhang, X.; Wang, L.; Wang, R.; Zhang, W.; Chen, C.; Zhang, W. Performance of Asphalt Mastic and Asphalt Mixture with Harmless Municipal Solid Waste Incineration Fly Ash. *Buildings* **2023**, *13*, 498. https://doi.org/10.3390/buildings13020498

Academic Editor: Ramadhansyah Putra Jaya

Received: 25 January 2023
Revised: 8 February 2023
Accepted: 9 February 2023
Published: 12 February 2023

Copyright: © 2023 by the authors. Licensee MDPI, Basel, Switzerland. This article is an open access article distributed under the terms and conditions of the Creative Commons Attribution (CC BY) license (https://creativecommons.org/licenses/by/4.0/).

1. Introduction

Municipal solid waste incineration fly ash (MSWIFA) is the waste product of the flue gas purification system and the bottom ash settles at the bottom of the flue and chimney during the incineration and disposal of municipal domestic waste. China's annual domestic garbage incineration capacity is about 140 million tons, and the volume of total ash generated can reach 4–5% of the total volume of garbage. The total mass of ash can reach 15–20% of the total mass of garbage, and the quantity of MSWIFA can reach 10–20% of the total mass of ash [1,2]. The moisture content of incineration MSWIFA is very low; it is a light grey powder consisting of particles of uneven size, with a complex structure and variable properties [3]. Most MSWIFA particles exist in the form of amorphous and

polycrystalline polymer structures [4,5]. Generally, the particle size of MSWIFA is less than 100 μm [6]. The chemical elements of MSWIFA include Cl, Ca, K, Na, Si, Al, O, etc. [7]. The main chemical components are CaO, SiO_2, Al_2O_3, and Fe_2O_3 [7]. In addition, incineration MSWIFA often contains heavy metals, such as Hg, Cr, Pb, Cd, Cu, and Zn [8]. These heavy metals mainly exist in the form of aerosol particles and are concentrated on the surface of the MSWIFA particles. The MSWIFA also contains a small number of dioxins and furans, so it has a strong potential hazard. These pollutants can harm the health of animals, plants, and human beings by polluting water and soil [9]. Therefore, it is necessary to treat MSWIFA to render it harmless before utilization. At present, the common harmless treatment methods include chemical treatment, high-temperature treatment, and cement solidification [10]. The chemical treatment method refers to mixing MSWIFA with organic or inorganic chemicals to inhibit the dissolution of MSWIFA and reduce its toxicity [2,4,9]. The high-temperature treatment method refers to burning MSWIFA into a glassy state, thus melting toxic substances [5,8]. The principle of cement solidification is to use the setting ability of the cement to fix MSWIFA in cement products to achieve the fixation of toxic substances and prevent secondary pollution. At present, the treatment of fly ash to render it harmless is accomplished at a large industrial scale in China [10]. For example, Zhongjie Environmental Protection Technology Co., Ltd. (Beijing, China), Jiangsu Jinghuicheng Environmental Engineering Co., Ltd. (Wuxi, China), and other enterprises have a relatively complete capacity for the treatment of MSWIFA.

The most common way is to use H-MSWIFA in cement-based material products to replace some of the fly ash. There are also reports on the application of H-MSWIFA in compression-stabilized soil mass [11]. It is also possible to prepare an environment-friendly geopolymer from H-MSWIFA and red mud carbonization residue [12]. There are also reports that H-MSWIFA can be applied to cement-stabilized soil to exert its bonding ability [13]. In short, H-MSWIFA is used more and more widely. In view of the high cost of the treatment of MSWIFA, how to realize high-value applications of H-MSWIFA has become a difficult problem and stands in the way of the application of H-MSWIFA. In view of the small particle size of H-MSWIFA and the high similarity between its technical performance and mineral powder, replacing the mineral powder with H-MSWIFA and apply it in asphalt mixtures with high value has become a hot research topic [14–18]. This is of far-reaching significance to the construction of energy-saving and environment-friendly highway projects and the promotion of the sustainable development of the highway industry [19–22]. However, in view of the limited application of H-MSWIFA in asphalt mixtures, to date, the following problems remain unsolved in its large-scale application.

(1) The effect of harmless H-MSWIFA replacing some of the mineral powder on the viscosity of asphalt mastic at room temperature, viscosity at high temperature, tensile property at low temperature, and crack resistance at room temperature is not clear [23–25].
(2) After harmless H-MSWIFA replaces some of the mineral powder, it is necessary to study the effect on the performance of the asphalt mixture [26–29].

In view of this, H-MSWIFA was used to replace some of the mineral powder, and asphalt mastic was prepared with different F/A. CPT, rotational viscosity, low-temperature bending, and FSFET tests were carried out to evaluate the viscosity at room temperature, viscosity at high temperature, tensile property at low temperature, and crack resistance at room temperature of the asphalt mastic with different F/A and different H-MSWIFA replacement ratios. AC-13 samples with different F/A and different H-MSWIFA replacement ratios were prepared. The effects of F/A and different H-MSWIFA replacement ratios on the high-temperature stability, water stability, and low-temperature cracking resistance of the asphalt mixture were studied. The aim of this study is to provide a reference for the application of H-MSWIFA in asphalt mixture.

2. Materials and Experimental Design

2.1. Materials

The H-MSWIFA is produced by Zhongjielan Environmental Protection Technology Co., Ltd. (Beijing, China). The process of rendering the MSWIFA harmless is as follows: circulating gradient washing to remove soluble salt, water treatment, drying and transportation, and evaporation to separate mineral salts.

Circulating gradient washing to remove soluble salt and water treatment: the fly ash after cyclic gradient washing and chlorine removal is directly transported to the high-temperature section at the kiln end through a sealed pipeline. The dioxin contained is completely decomposed, and the heavy metal can be effectively fixed in the cement clinker lattice.

Drying and transportation, and evaporation to separate salt: After water treatment, the washed water is evaporated and crystallized to extract sodium potassium salt from the wastewater, and then made into industrial sodium chloride and potassium chloride. The evaporated water is recycled and returned to the system for reuse.

The elemental composition of the H-MSWIFA used in this study is shown in Table 1 and the technical indicators are shown in Table 2. The mineral powder is made by grinding limestone in the laboratory and its technical indicators are also shown in Table 2.

Table 1. Distribution of H-MSWIFA elements.

Element	O	Na	Mg	Si	Al	P	Cl	S	K	Ca	Other
Proportion, %	27.66	3.11	0.78	0.99	0.47	0.24	20.76	1.75	4.65	38.18	1.66

Table 2. Technical performance of H-MSWIFA and mineral powder.

Technical Indicators		H-MSWIFA	*CV*	Mineral Powder	*CV*	Test Method [30]
Hydrophilicity coefficient		0.69	0.031	0.71	0.042	T 0353
Plasticity index, %		3.6	0.065	3.5	0.091	T 0353
Size range, %	<0.6 mm	100	0.023	100	0.066	T 0351
	<0.15 mm	96.4	0.029	91.8	0.070	T 0351
	<0.075 mm	92.5	0.063	88.2	0.081	T 0351

The asphalt used in this study is "Donghai" road asphalt, produced by China Petrochemical Corporation (Beijing, China), and its technical indicators are shown in Table 3. The aggregate is basalt aggregate and its technical indicators are shown in Table 4.

Table 3. Technical indicators of asphalt.

Technical Indicators		Asphalt				Test Method [31]
		SBS I-C	*CV*	90A	*CV*	
Penetration (25 °C, 100 g, 5 s), 0.1 mm		75.7	0.029	91.6	0.052	T 0604
PI		0.98	0.074	−0.89	0.087	T 0604
Softening point (globe method), °C		≥80.1	0.091	46.7	0.024	T 0606
Ductility (5 °C, 5 cm/min), cm		41.8	0.041	——	0.07	T 0605
Ductility (10 °C, 5 cm/min), cm		>100	0.065	>100	0.057	T 0605
Ductility (15 °C, 5 cm/min), cm		>100	0.024	>100	0.027	T 0605
Dynamic viscosity at 60 °C, Pa.s		——	0.05	182.4	0.051	T 0619
Kinematic viscosity at 135 °C, Pa.s		1.812	0.063	——	0.056	T 0625
Flashpoint, °C		327	0.07	331	0.062	T0611
Solubility, %		99.85	0.026	99.87	0.09	T0607
Density (15 °C), g/cm^3		1.004	0.023	1.033	0.043	T0603
Wax content, %		——	0.09	1.6	0.03	T0615
Elastic recovery (25 °C), %		95.1	0.086	——	0.015	T0662
Segregation, 48 h softening point difference, °C		0.7	0.06	——	0.068	T0661
RTFOT [1] 163 °C, 5 h	Quality change, %	0.011	0.094	−0.077	0.018	T0610
	Residual penetration ratio, %	78.4	0.035	70.2	0.093	T0604
	Residual ductility (10 °C), cm	25.3	0.017	15.3	0.038	T0605

[1] RTFOT: Rolling Thin Film Oven Test. SBS I-C: Styrene–Butadiene–Styrene Block Copolymer modified asphalt with quality grade I-C. 90A: Grade A asphalt with a median penetration of 90 (0.1 mm).

Table 4. Technical indicators of Aggregate.

Aggregate Type	Technical Indicators	Measured Value	*CV*	Test Method [30]
Coarse aggregate	Crushing value, %	10.1	0.067	T 0316
	Los Angeles abrasion loss, %	8.4	0.040	T 0317
	Water absorption, %	0.36	0.032	T 0307
	Soundness, %	7.7	0.089	T 0314
	Needle and flaky content, %	5.6	0.053	T 0312
Fine aggregate	Soundness, %	8.0	0.038	T 0340
	Mud content, %	1.4	0.064	T 0335
	Sand equivalent, %	74.8	0.066	T 0334
	Methylene blue value, g/kg	14.4	0.090	T 0349
	Angularity, s	17.3	0.051	T 0345

2.2. Experimental Design

In this paper, H-MSWIFA is used to replace some of the mineral powder, and the replacement ratio is 0%, 25%, 50%, 75%, and 100% respectively. Asphalt mastics are then prepared with F/A ratios of 0.6, 0.8, 1.0, 1.2, and 1.4 respectively. The specific preparation process is as follows. A sample of 90A asphalt is heated to 150 °C, and the H-MSWIFA and mineral powder are mixed according to the corresponding replacement ratio, and then heated to 140 °C. A certain amount of H-MSWIFA and mineral powder are added into the asphalt slowly according to the established F/A, and a mixing rod is used to ensure even mixing. A high-speed shearing instrument is then used to shear at a speed of 1000 r/min for 5 min, then at a speed of 3000 r/min for 10 min, and finally, at a speed of 1000 r/min for 5 min to prepare H-MSWIFA asphalt mastic. The asphalt mastic should be used as soon as possible after preparation to avoid deposition of H-MSWIFA and mineral powder resulting in interference with the test results caused by long-term placement.

CPT, rotational viscosity, low-temperature bending, and FSFET tests on the prepared H-MSWIFA asphalt (90A) mastics were carried out to evaluate the viscosity at room temperature, viscosity at high temperature, tensile property at low temperature, and crack resistance at room temperature of the asphalt mastic with different F/A and different H-MSWIFA replacement ratios. AC-13 samples with different H-MSWIFA replacement ratios and F/A were prepared with SBS I-C, H-MSWIFA, mineral powder, basalt aggregate, etc. Dynamic Stability (DS), Maximum bending and tensile strain (ε_B), Residual Marshall Stability (MS'), and Frozen-Thaw and Split Residual Strength Ratio (TSR) tests were carried out to detect the high-temperature stability, low-temperature cracking resistance, and water stability of H-MSWIFA asphalt mixture, respectively.

3. The Performance H-MSWIFA Asphalt Mastic

3.1. Analysis of CPT Results

CPT is a test method specially used to evaluate the viscosity of asphalt mastic at room temperature. It is an improvement of the asphalt penetration test. The long needle of the penetration is replaced by a cone needle, and the size of the sample container is increased [31,32]. The cone needle for cone penetration is shown in Figure 1. It is made of stainless steel and can carry a certain weight according to the experimental requirements. The dimensions of the stainless steel sample container are diameter, 70 mm, and depth, 50 mm. The procedure for CPT is largely the same as the asphalt penetration test method. The freshly prepared asphalt mastic is poured into the sample container such that the sample height reaches 2/3 of the container depth, after cooling at room temperature, the container is placed in water (25 °C) for 2.5 h, and then CPT is conducted according to the asphalt penetration test method. The test result is accurate to 0.1 mm.

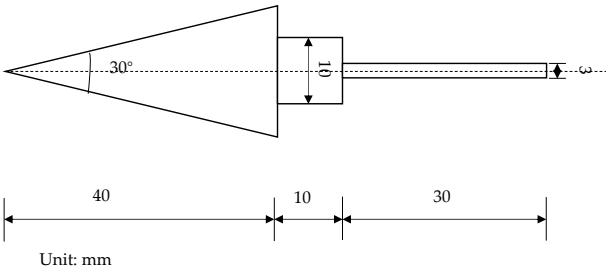


Figure 1. Dimensions of the CPT cone needle.

According to the CPT results, the shear strength of an asphalt mastic can also be calculated as shown in Equation (1).

$$\tau = \frac{981Q\cos^2(\alpha/2)}{\pi h^2 \tan^2(\alpha/2)} \quad (1)$$

where τ is shear strength, KPa; Q is penetration mass (total mass of cone needle, connecting rod, and method), g, 1950.685 g in this paper; H is cone penetration, 0.1 mm; and α is the cone needle tip angle, 30° in this paper.

In this paper, CPT at 25 °C had been carried out for asphalt mastics with different F/A and H-MSWIFA replacement ratios. The test results are shown in Figure 2.

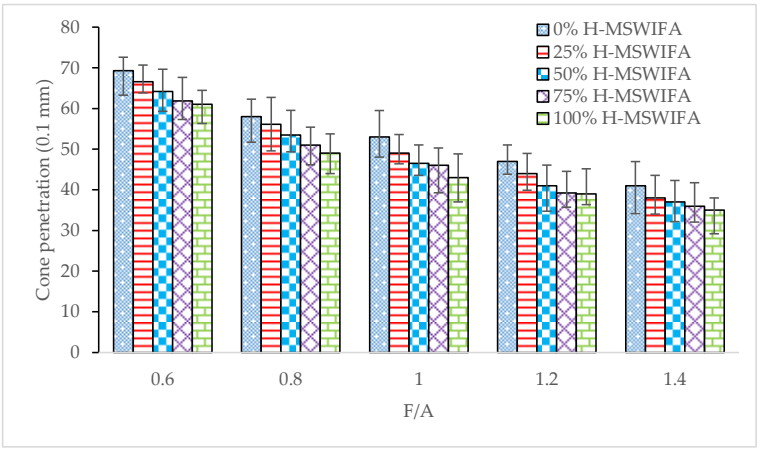


Figure 2. CPT results.

Figure 2 shows that, for asphalt mastics with the same H-MSWIFA replacement ratios, the greater the F/A, the smaller the cone penetration of the asphalt mastic, Taking the cone penetration of asphalt mastic with a F/A of 0.6 as the reference value, under the same H-MSWIFA replacement ratio, when the F/A is 0.8, 1.0, 1.2, and 1.4, the cone penetration of the asphalt mastic is about 80~85%, 10~76%, 63~68%, and 57~59% of the reference value. The cone penetration of asphalt mastics with different H-MSWIFA replacement ratios is gradually reduced with the gradual increase in replacing ratio, but the decrease is relatively small compared with the F/A. Taking the H-MSWIFA replacement ratio of 0% as the reference value, when the F/A is 0.6, the cone penetration of the asphalt mastics with the H-MSWIFA replacement ratio of 25%, 50%, 75%, and 100% is 96%, 93%, 89% and 88% of the reference value respectively. When the F/A is 0.8, this ratio is 96%, 92%, 88%, and 84% respectively. When the F/A is 1.0/1.2/1.4, this ratio is 92%/94%/93%, 88%/87%/90%, 87%/83%/88%, and 81%/82%/85% respectively. It can be seen that the viscosity of the asphalt mastic is improved after H-MSWIFA replaces some of the mineral powder, which is related to the smaller particle size and larger pH value of H-MSWIFA.

The asphalt mastic shear strength at 25 °C is shown in Table 5.

Table 5. Shear strength calculation results.

H-MSWIFA Replacement Ratio, %	Shear Strength of Ratio Of Filler Asphalt (KPa)				
	0.6	**0.8**	**1**	**1.2**	**1.4**
0	44.2	63.1	75.5	96.0	126.2
25	47.8	67.4	88.3	109.6	146.9
50	51.5	74.1	98.1	126.2	154.9
75	55.4	81.5	100.2	138.0	163.7
100	57.0	88.3	114.7	139.4	173.1

With the increase in the H-MSWIFA replacement ratio, the shear strength with the same F/A increases correspondingly, but the increase is limited. However, the change in the F/A has a great impact on the shear strength. For asphalt mastics with the same H-MSWIFA replacement ratio, the shear strength at a F/A of 1.4 is about three times that at a F/A of 0.6. This rule can also be explained by Equation (1). In conclusion, it can be concluded that the shear strength increases after H-MSWIFA replaces some of the mineral powder. At the same time, the greater the F/A, the greater the shear strength.

3.2. Analysis of Rotational Viscosity Test Results

Asphalt mastics were prepared with H-MSWIFA replacement ratios of 0%, 25%, 50%, 75%, and 100%, and F/A of 0.6, 0.8, 1.0, 1.2, and 1.4 respectively. The rotational viscosity of asphalt mastic at 135 °C was measured by using a rotational viscometer as shown in Figure 3.

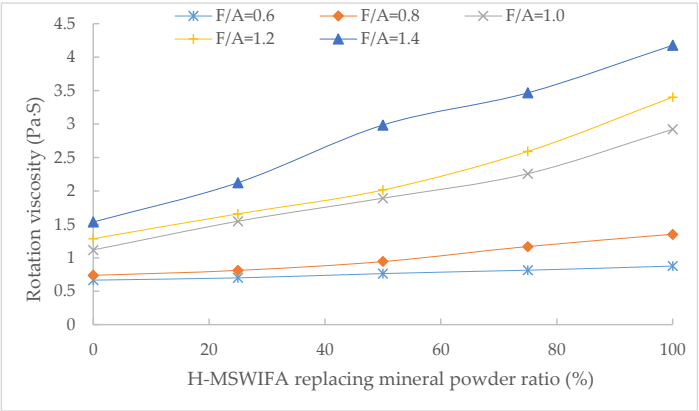


Figure 3. Rotational viscosity test results of asphalt mastics.

The rotational viscosity at 135 °C of asphalt mastics with different H-MSWIFA replacement ratios is different, and the rotational viscosity increases with the increase in the H-MSWIFA replacement ratio. This rule is not obvious when F/A is 0.6 and 0.8, but it becomes very significant when F/A is 1.0 and above. Taking a F/A of 1.2 as an example, when the H-MSWIFA replacement ratio is 25%, 50%, 75%, and 100%, the rotational viscosity of asphalt mastic is 2.6 times the 1.3, 1.6, and 2.0 grades when the H-MSWIFA replacement ratio is 0%. This further shows that H-MSWIFA can greatly improve the viscosity of asphalt mastic at high temperatures.

3.3. Analysis of Low-Temperature Bending Test Results of Asphalt Mastic

Some scholars have applied this test to the determination of the low-temperature tensile properties of asphalt mastic. The test results can well reflect the low-temperature tensile properties and have been unanimously recognized by the construction industry [32–36]. The asphalt mastic was prepared with H-MSWIFA replacement ratios of 0%, 25%, 50%, 75%, and 100%, and F/A of 0.6, 0.8, 1.0, 1.2, and 1.4, respectively. This is then poured into the test mold with an inner diameter of 40 mm × 40 mm × 140 mm, which is placed on a

horizontal plate after natural cooling and kept for 2.5 h at −10 °C. The support of the test piece of the press is adjusted to ensure that the span of the test piece is 125 mm ± 0.5 mm, and then it is loaded at −10 °C with single-point loading at a loading rate of 5 mm/min. During this test, the stress and strain values of the test piece are collected, and the bending stiffness modulus (S_B), flexural strength (R_B), and maximum bending and tensile strain (ε_B) are obtained and calculated when the test piece is damaged. The calculation equations of R_B, $\varepsilon_{B,}$ and S_B are shown in Equations (2) to (4).

$$R_B = \frac{3LP_B}{2bh^2} \tag{2}$$

$$\varepsilon_B = \frac{6hd_0}{L^2} \tag{3}$$

$$S_B = \frac{R_B}{\varepsilon_B} \tag{4}$$

where b is the width in the middle of the test piece, mm; h is the height in the middle of the test piece, mm, mm; L is the span of the test piece, mm; P_B is the maximum load when the test piece is damaged, N; d_0 is the midspan deflection when the test piece is damaged, mm.

The test results are shown in Figures 4–6.

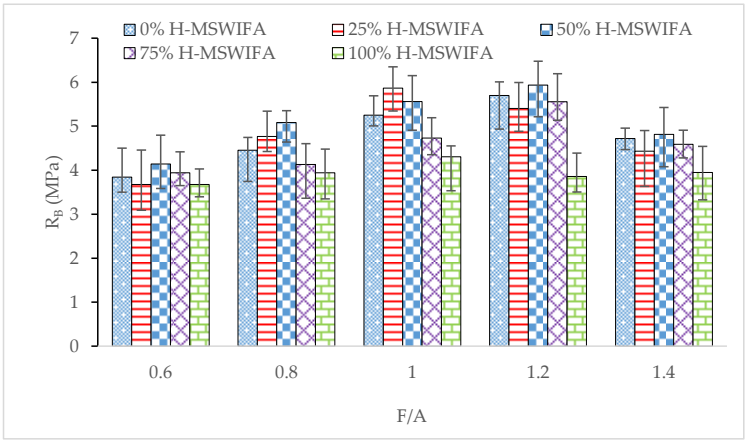


Figure 4. Test results of R_B.

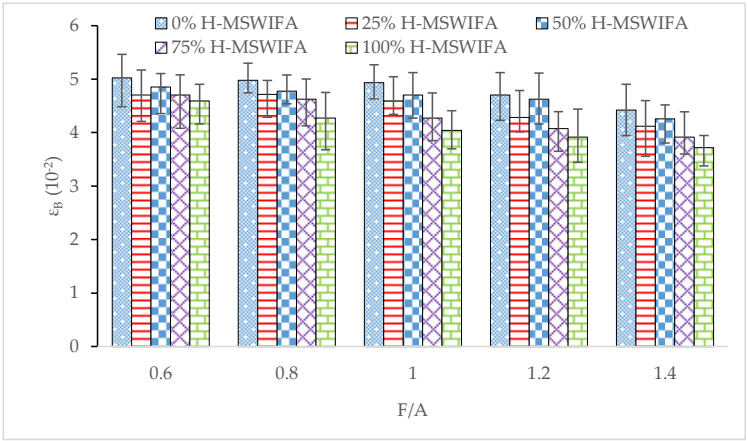


Figure 5. Test results of ε_B.

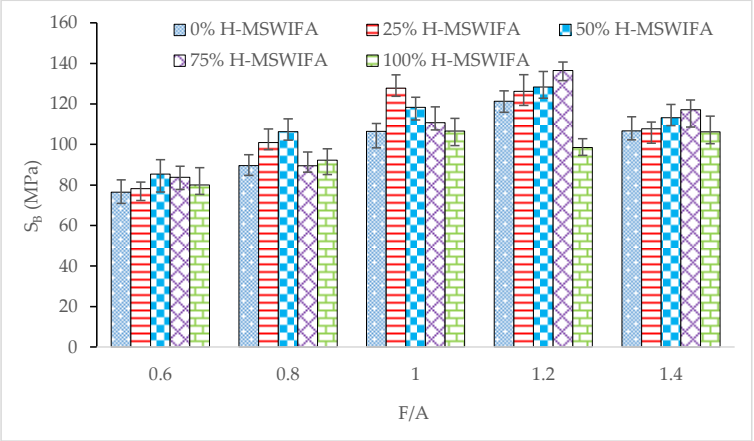


Figure 6. Test results of S_B.

Figure 4 shows that the R_B of the test piece first increases and then decreases with the increase in F/A, reaching a maximum at the point where F/A is 1.0 or 1.2. This rule is consistent for all H-MSWIFA replacement ratios. For different H-MSWIFA replacement ratios, the R_B of the asphalt mastic test piece changes with the change in replacement ratio. When the replacement ratio is about 50%, the RB of asphalt mastic with the same F/A is the largest. Figure 5 shows the ε_B decreases with the decrease in asphalt mastic F/A and the increase in the H-MSWIFA replacement ratio. Figure 6 shows the relationship between S_B and F/A, and the relationship between S_B and H-MSWIFA replacement ratio, which is similar to the relationship between R_B and F/A or H-MSWIFA replacement ratio. This phenomenon shows that the addition of H-MSWIFA has an adverse effect on the low-temperature performance of the asphalt mastic. From the perspective of controlling the low-temperature performance of asphalt mastic, the H-MSWIFA replacement ratio should not be too high.

3.4. Analysis of FSFET Results

FSFET can obtain the stress-real strain on the central full fracture surface at room temperature, allowing an accurate full-section fracture energy (FSFE) to be obtained [37]. The test is carried out with reference to the Direct Tensile (DT) test. In theory, the DT test is an appropriate method to obtain asphalt fracture energy. However, because the middle part of the DT sample is too long, the tensile stress in this part is consistent, and cracking may occur anywhere in this part, resulting in an inability to obtain the true strain on the failure surface. In addition, the error generated during asphalt pouring means that stress concentration readily occurs in the area with reduced cross-section, which leads to failure and fracture. For some asphalts with large ductility, the loading rate of DT test equipment cannot meet the requirements of the room temperature fracture test. Therefore, scholars have improved the DT specimen model to keep the stress concentration of the specimen consistent in the middle cross-section [37]. MTS is used as the tensile test equipment to obtain different tensile rates and test temperatures and to test the FSFE of asphalt at a constant temperature.

On this basis, this paper applies the method to the study of asphalt mastics. The test rate is 500 mm/min at 15 °C, and. In this paper, asphalt mastics were prepared with H-MSWIFA replacement ratios of 0%, 25%, 50%, 75%, and 100%, and F/A of 0.6, 0.8, 1.0, 1.2, and 1.4. Six test pieces are prepared for each type of asphalt mastic, and the representatives of each working condition are shown in Figures 7–11.

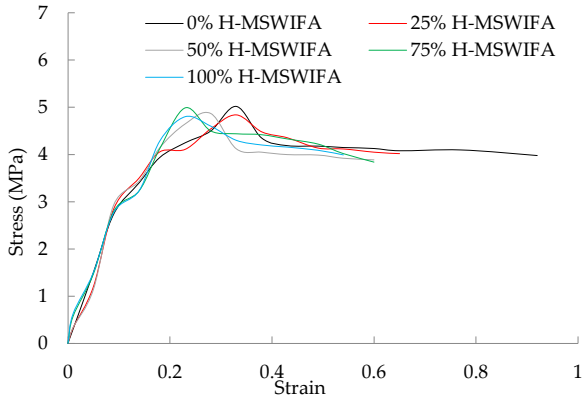


Figure 7. FSFE curve of asphalt mastic at F/A of 0.6.

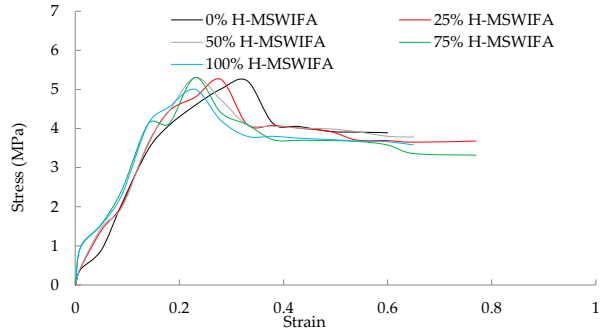


Figure 8. FSFE curve of asphalt mastic at F/A of 0.8.

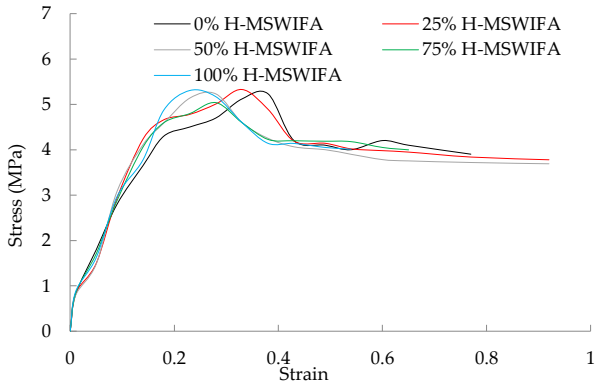


Figure 9. FSFE curve of asphalt mastic at F/A of 1.0.

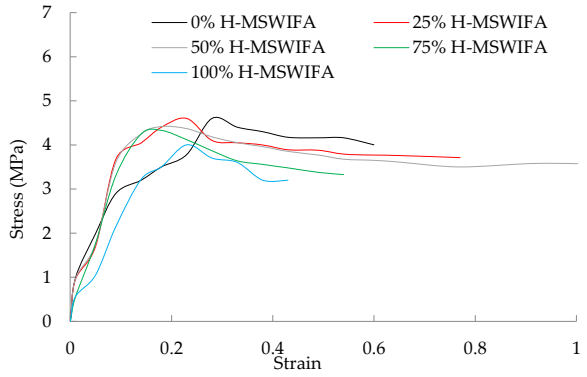


Figure 10. FSFE curve of asphalt mastic at F/A of 1.2.

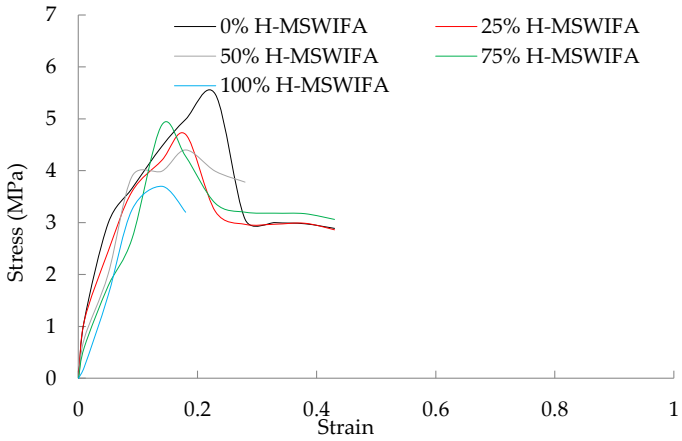


Figure 11. FSFE curve of asphalt mastic at F/A of 1.4.

Figures 7–11 show that during the FSFE, the stress-strain curves of asphalt mastics under different working conditions are similar, and the stress gradually increases with the increase in strain. After reaching the maximum stress value, the stress decreases rapidly until fracture with the continuous increase in strain. The specific performances of the full-section fracture test curves of asphalt mastics with different H-MSWIFA replacement ratios differ. When F/A is fixed, the maximum stress value of asphalt mastic during the test gradually decreases with the gradual increase in the H-MSWIFA replacement ratio, or the strain corresponding to the maximum stress decreases when the maximum stress value is similar. The calculation results of the FSFE of each specimen are summarized in Table 6.

Table 6. FSFE results of asphalt mastics.

H-MSWIFA Replacement Ratio, %	No.	Calculated Value of FSFE Density with Different F/A, MPa				
		0.6	**0.8**	**1**	**1.2**	**1.4**
0	1	1.73	1.54	1.22	1.16	0.91
	2	1.58	1.6	1.37	1.15	1.13
	3	1.62	1.64	1.45	1.13	1.01
	4	1.59	1.47	1.44	1.03	1.18
	5	1.64	1.49	1.23	0.99	1.07
	6	1.66	1.58	1.24	1.29	1.09
	average value	1.637	1.553	1.325	1.125	1.065
	CV	0.033	0.042	0.081	0.094	0.089
25	7	1.67	1.54	1.39	1.27	1.14
	8	1.73	1.66	1.21	1.37	1.23
	9	1.66	1.43	1.32	1.46	1.34
	10	1.79	1.72	1.36	1.13	1.02
	11	1.68	1.69	1.48	1.16	1.08
	12	1.62	1.74	1.27	1.05	1.23
	average value	1.69	1.63	1.34	1.24	1.17
	CV	0.035	0.074	0.0706	0.126	0.099
50	13	2.06	1.8	1.41	1.27	1.37
	14	1.95	1.86	1.44	1.45	1.16
	15	2.17	1.69	1.45	1.33	1.34
	16	2.14	1.85	1.48	1.38	1.02
	17	2.07	1.6	1.57	1.44	1.13
	18	2.05	1.65	1.31	1.26	1.31
	average value	2.07	1.74	1.44	1.36	1.22
	CV	0.037	0.063	0.059	0.060	0.1138

Table 6. *Cont.*

H-MSWIFA Replacement Ratio, %	No.	Calculated Value of FSFE Density with Different F/A, MPa				
		0.6	**0.8**	**1**	**1.2**	**1.4**
75	19	1.33	1.12	1.08	0.65	0.58
	20	1.16	0.85	0.99	0.89	0.63
	21	1.45	0.91	0.72	0.69	0.76
	22	1.18	1.06	1.09	0.84	0.73
	23	1.48	1.19	0.96	0.81	0.59
	24	1.17	1.02	0.77	0.62	0.54
	average value	1.30	1.03	0.94	0.75	0.64
	CV	0.1127	0.124	0.167	0.162	0.1378
100	25	0.99	0.97	0.67	0.67	0.55
	26	0.93	0.88	0.84	0.47	0.53
	27	1.17	0.85	0.82	0.5	0.46
	28	1.21	0.74	0.76	0.56	0.49
	29	0.86	0.7	0.79	0.54	0.39
	30	0.85	0.98	0.77	0.69	0.35
	average value	1.00	0.85	0.78	0.57	0.46
	CV	0.154	0.135	0.1768	0.157	0.170

Table 6 shows that for asphalt mastics with the same F/A, with the gradual increase in the H-MSWIFA replacement ratio, the FSFE of the asphalt mastic first increases and then decreases, reaching a maximum when the H-MSWIFA replacement ratio is 50%. For the asphalt mastic with the same H-MSWIFA replacing the mineral powder ratio, its FSFE decreases rapidly with the increase in the F/A. This shows that H-MSWIFA can improve the anti-cracking performance of asphalt mastic at room temperature to a certain extent by replacing part of the mineral powder, but when the replacement rate exceeds 50%, the anti-cracking performance at room temperature will be rapidly reduced. In addition, the larger the F/A, the smaller the anti-cracking performance of asphalt mastic at room temperature. Therefore, from the perspective of cracking resistance of asphalt mastic at room temperature, the H-MSWIFA replacement ratio should not be too high, and should not be higher than 50%, and the F/A should not be too large.

4. The Performances of H-MSWIFA Asphalt Mixture

AC-13 with different F/A and different H-MSWIFA replacement ratios were prepared with SBS I-C, H-MSWIFA, mineral powder, and basalt aggregate. Then the DS, ε_B, MS', and TSR were tested to evaluate the high-temperature stability, low-temperature cracking resistance, and water stability of the H-MSWIFA asphalt mixture, respectively. In this paper, the Marshall volume design method is used to design the asphalt mixtures. The test of DS adopts a 300 mm × 300 mm × 50 mm test piece formed by the wheel rolling method, with a wheel width of 300 mm and a compaction line load of 300 N/cm. At 155 °C, the test piece can be made after 4 times preloading and then 24 times rolling. The prepared test piece can be cut after cooling to obtain the specified 250 mm × 30 mm × 35 mm small beam for ε_B, and the loading rate during the test is 50 mm/min. The test pieces used by TSR and MS' are Marshall test pieces, with a diameter of 106.6 mm and a height of 63.5 mm. They are made by lifting a flat circular indenter with a diameter of 98.5 mm to a height of 457.2 mm, and free-falling compaction. The test piece for the TSR test is obtained by 50 repeats of double-sided compaction, while the test piece for the MS' test is obtained by 75 repeats of double-sided compaction. In order to avoid interference from the gradation to the test results, the gradation of AC-13 is unified in this paper, as shown in Figure 12. Considering the influence of the F/A, the asphalt-aggregate ratio is fixed at 5.0%. Partial mix design data of the H-MSWIFA asphalt mixture are shown in Table 7, and the measurement method of the volume parameters is the water weight method.

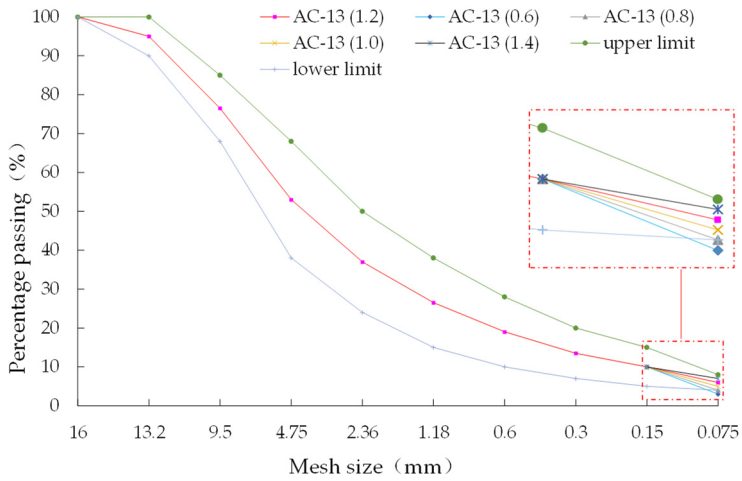


Figure 12. The Grading Curve of AC-13.

Table 7. Partial mix design data of the H-MSWIFA asphalt mixture (AC-13).

F/A	Mix Design Data	H-MSWIFA Replacement Ratio									
		0		25		50		75		100	
		Value	*cv*	Value	*cv*	Value	*cv*	Value	*cv*	Value	*cv*
0.6	VV	3.62	0.064	3.89	0.082	3.7	0.085	3.79	0.047	3.63	0.058
	MS	8.3	0.129	5.5	0.112	5.4	0.131	7.5	0.142	7.9	0.148
0.8	VV	3.74	0.087	3.72	0.081	3.51	0.084	3.75	0.065	3.83	0.072
	MS	8.1	0.088	9.9	0.157	8.3	0.162	7.4	0.138	7.2	0.119
1.0	VV	3.57	0.038	3.54	0.068	3.75	0.071	3.72	0.09	3.82	0.042
	MS	8.1	0.161	8.9	0.101	9.9	0.172	0.123	0.128	9.2	0.164
1.2	VV	3.53	0.052	3.91	0.089	3.59	0.061	3.66	0.05	3.69	0.057
	MS	9.2	0.16	9.4	0.156	10.7	0.094	11.8	0.134	11.3	0.159
1.4	VV	3.83	0.083	3.97	0.034	3.8	0.068	3.64	0.04	3.87	0.068
	MS	10.3	0.141	10.9	0.129	11.3	0.111	12.6	0.136	12.7	0.167

The rutting test of AC-13 with different F/A and different H-MSWIFA replacement ratios was carried out to obtain the DS. The test results are summarized in Figure 13.

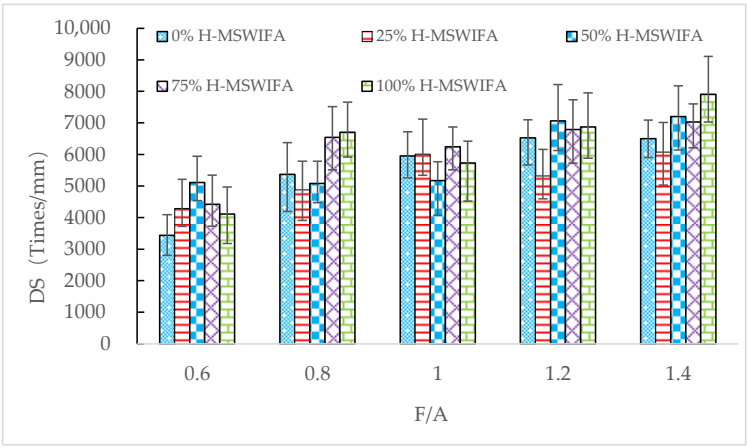


Figure 13. The DS of AC-13.

Figure 13 shows that the DS of AC-13 increases significantly with the increase in the F/A, which is applicable to all H-MSWIFA replacement ratios. However, for AC-13 with a fixed F/A, the effect of the H-MSWIFA replacement ratio on DS does not show a certain

rule. This shows that the high-temperature stability has little to do with the replacement of mineral powder by H-MSWIFA but mainly depends on the value of F/A.

Immersion Marshall and freeze-thaw splitting tests of AC-13 with different F/A and different H-MSWIFA replacement ratios were carried out to obtain the MS′ and TSR. The test results are summarized in Figures 14 and 15.

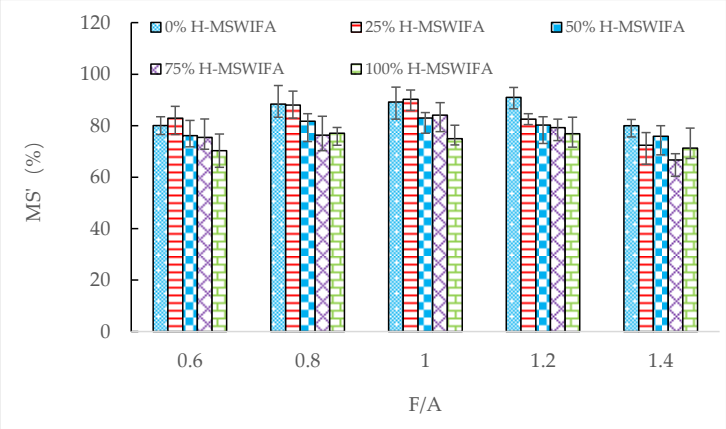


Figure 14. The MS′ of AC-13.

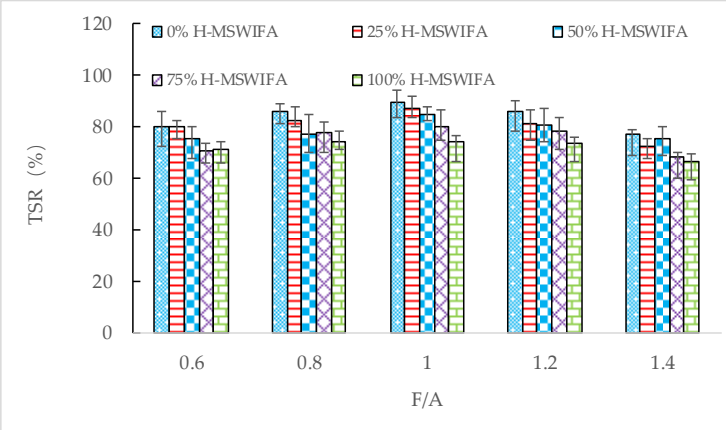


Figure 15. The TSR of AC-13.

The MS′ and TSR are both evaluation indicators of the water stability of asphalt mixtures. It can be seen from Figures 14 and 15 that the F/A and the H-MSWIFA replacement ratio have a certain impact on the test results. Specifically, when the H-MSWIFA replacement ratio is fixed, MS′ and TSR first increase and then decrease rapidly with the increase in F/A and reach a maximum near a F/A of 1.0. When F/A is fixed, MS′ and TSR gradually decrease with the increase in the H-MSWIFA replacement ratio. This phenomenon shows that the water stability of the asphalt mixture can be significantly affected by the F/A and the H-MSWIFA replacement ratio. The specific performance is that the water stability reaches the best value when F/A is around 1.0, and the addition of H-MSWIFA can harm water stability. From the perspective of water stability, the H-MSWIFA replacement ratio should not be too high.

Low-temperature bending tests of AC-13 with different F/A and different H-MSWIFA replacement ratios were carried out to obtain the ε_B. The test results are summarized in Figure 16.

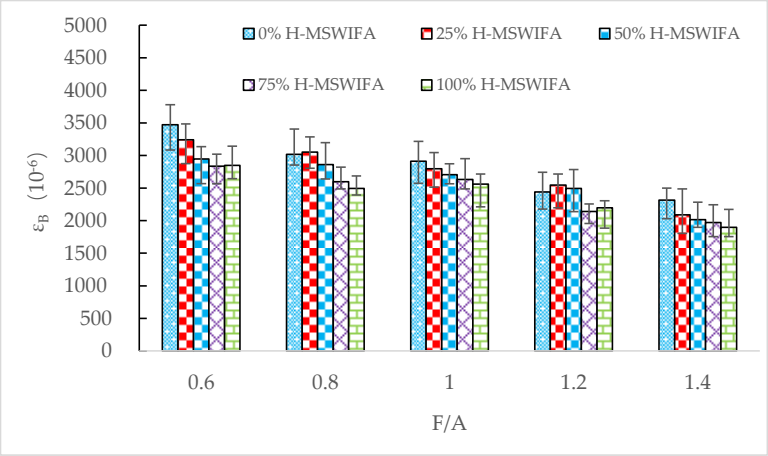


Figure 16. The ε_B of AC-13.

ε_B as an evaluation index of low-temperature crack resistance of asphalt mixtures, the larger the value, the stronger the low-temperature crack resistance of the asphalt mixture. It can be seen from Figure 16 that the F/A and the H-MSWIFA replacement ratio have a certain impact on the test results. Specifically, when the H-MSWIFA replacement ratio is fixed, ε_B decreases rapidly with the increase in F/A, and when F/A is fixed, the value of ε_B also shows a decreasing trend with the increase in the H-MSWIFA replacement ratio. This phenomenon shows that both the F/A and H-MSWIFA replacement ratio can significantly affect the low-temperature anti-cracking performance of the asphalt mixture. The higher the F/A, the worse the low-temperature anti-cracking performance of the asphalt mixture. At the same time, the addition of H-MSWIFA harms low-temperature anti-cracking performance. From the perspective of low-temperature anti-cracking performance, the H-MSWIFA replacement ratio should not be too high.

5. Conclusions

This paper has studied the performance of asphalt mastic and asphalt mixture with H-MSWIFA replacing fly ash, and the conclusions are as follows.

(1) The shear strength and viscosity of asphalt mastic increased after H-MSWIFA replaced some of the mineral powder; At the same time, the greater the F/A, the greater the shear strength and viscosity of the asphalt mastic. H-MSWIFA can also improve the viscosity of asphalt mastic at high temperatures.
(2) From the point of view of the cracking resistance of asphalt mastic at room temperature, the H-MSWIFA replacement ratio should not be too high—not more than 50%—and the F/A should not be too large.
(3) The high-temperature stability of the asphalt mixture is not related to the H-MSWIFA replacement ratio but mainly depends on the F/A.
(4) Both the F/A and the H-MSWIFA replacement ratio can significantly affect the water stability and the low-temperature cracking resistance of the asphalt mixture. Specifically, water stability reaches the best value when the F/A is around 1.0, and the higher the F/A, the worse the low-temperature crack resistance.
(5) The addition of H-MSWIFA harms water stability and low-temperature cracking resistance. From the perspective of water stability and low-temperature cracking resistance, the H-MSWIFA replacement ratio should not be too high.

Author Contributions: Conceptualization, X.Z. and W.Z. (Wei Zhang); Data curation, L.W., R.W. and W.Z. (Wengang Zhang); Formal analysis, L.W.; Funding acquisition, W.Z. (Wei Zhang) and C.C.; Investigation, X.Z. and C.C.; Methodology, E.L., X.Z. and L.W.; Project administration, W.Z. (Wei Zhang) and C.C.; Resources, R.W. and W.Z. (Wei Zhang); Software, E.L. and R.W.; Validation, X.Z.; Writing—original draft, E.L. and W.Z. (Wengang Zhang) All authors have read and agreed to the published version of the manuscript.

Funding: This research was funded by "The Fundamental Research Funds for Gansu Province Educational Technology Innovation Project", grant number 2022B-063, "The Fundamental Research Funds for the Central Universities", grant number 31920220126, "The Fundamental Research Funds for the Central Universities", grant number 31920200060 and 31920200033.

Informed Consent Statement: Not applicable.

Data Availability Statement: Not applicable.

Conflicts of Interest: The authors declare no conflict of interest.

References

1. Liu, J.; Wang, Z.D.; Xie, G.M.; Li, Z.L.; Fan, X.; Zhang, W.Z.; Xing, F.; Tang, L.P.; Ren, J. Resource utilization of municipal solid waste incineration fly ash-cement and alkali-activated cementitious materials: A review. *Sci. Total Environ.* **2022**, *852*, 158254. [CrossRef] [PubMed]
2. Shang, N.; Wang, H.Y.; Wu, H.N.; Ko, J.H.; XV, Q.Y. Study of compressive strength and leachability of cement mortars containing municipal solid waste incineration fly ash. *Chin. J. Environ. Eng.* **2016**, *10*, 3207–3214. (In Chinese)
3. Lu, N.; Ran, X.; Pan, Z.; Korayem, A.H. Use of Municipal Solid Waste Incineration Fly Ash in Geopolymer Masonry Mortar Manufacturing. *Materials* **2022**, *15*, 8689. [CrossRef] [PubMed]
4. Wang, C.; Zhang, P.; Guo, J.; Zhang, H.; Wang, T. Effect of Municipal Solid Waste Incineration Ash on Microstructure and Hydration Mechanism of Geopolymer Composites. *Buildings* **2022**, *12*, 723. [CrossRef]
5. Cao, X.; Zhang, Q.S.; Yang, W.C.; Fang, L.; Liu, S.W.; Ma, R.; Guo, K.; Ma, N. Lead-chlorine synergistic immobilization mechanism in municipal solid waste incineration fly ash (H-MSWIFA)-based magnesium potassium phosphate cement. *J. Hazard. Mater.* **2023**, *442*, 130038. [CrossRef]
6. Zheng, R.F.; Wang, Y.; Liu, Z.X.; Zhou, J.Z.; Yue, Y.; Qian, G.R. Environmental and economic performances of municipal solid waste incineration fly ash low-temperature utilization: An integrated hybrid life cycle assessment. *J. Clean. Prod.* **2022**, *340*, 130680. [CrossRef]
7. Ren, P.F.; Ling, T.C.; Mo, K.H. CO_2 pretreatment of municipal solid waste incineration fly ash and its feasible use as supplementary cementitious material. *J. Hazard. Mater.* **2022**, *424*, 127457. [CrossRef]
8. Ren, P.F.; Ling, T.C. Roles of chlorine and sulphate in H-MSWIFA in GGBFS binder: Hydration, mechanical properties and stabilization considerations. *Environ. Pollut.* **2021**, *284*, 117175. [CrossRef]
9. Shiota, K.; Nakamura, T.; Takaoka, M.; Aminuddin, S.F.; Oshita, K.; Fujimori, T. Stabilization of cesium in alkali-activated municipal solid waste incineration fly ash and a pyrophyllite-based system. *Chemosphere* **2017**, *187*, 188–195. [CrossRef]
10. Wang, Y.; Ni, W.; Suraneni, P. Use of Ladle Furnace Slag and Other Industrial By-Products to Encapsulate Chloride in Municipal Solid Waste Incineration Fly Ash. *Materials* **2019**, *12*, 925. [CrossRef]
11. Abinaya, T.L.; Balasubramanian, M. A Circular Economy in Waste Management Carrying Out Experimental Evaluation Of Compressed Stabilized Earth Block Using Municipal Solid Waste Incinerator Fly Ash. *J. Eng. Res.* **2022**, *10*, 16319. [CrossRef]
12. Bai, Y.; Guo, W.C.; Wang, X.L.; Pan, H.M.; Zhao, Q.X.; Wang, D.L. Utilization of municipal solid waste incineration fly ash with red mud-carbide slag for eco-friendly geopolymer preparation. *J. Clean. Prod.* **2022**, *340*, 130820. [CrossRef]
13. Liang, S.H.; Chen, J.T.; Guo, M.X.; Feng, D.L.; Liu, L.; Qi, T. Utilization of pretreated municipal solid waste incineration fly ash for cement-stabilized soil. *Waste Manag.* **2020**, *105*, 425–432. [CrossRef]
14. Li, C.C.; Liu, Q.; Lei, J.; Zhang, Z.Y.; Fu, C.L.; Pan, F. Influence of mineral fillers properties on the bonding properties of bitumen mastics. *Constr. Build. Mater.* **2022**, *318*, 126013. [CrossRef]
15. Mukhtar, N.; Hasan, M.R.M.; Ghazali, M.F.H.M.; Zin, Z.M.; Shariff, K.A.; Sani, A. Influence of concentration and packing of filler particles on the stiffening effect and shearing behaviour of asphalt mastic. *Constr. Build. Mater.* **2021**, *295*, 123660. [CrossRef]
16. Wang, F.; Xiao, Y.; Chen, Z.W.; Cui, P.D.; Liu, J.; Wang, N. Morphological characteristics of mineral filler and their influence on active adhesion between aggregates and bitumen. *Constr. Build. Mater.* **2022**, *323*, 126520. [CrossRef]
17. Maia, M.M.A.S.; Dinis-Almeida, M.; Martinho, F.C.G. The Influence of the Affinity between Aggregate and Bitumen on the Mechanical Performance Properties of Asphalt Mixtures. *Materials* **2021**, *14*, 6452. [CrossRef]
18. Zhang, W.; Zou, L.; Chen, F.; Yang, C.; Li, Y.; Yan, X.; Zang, J.H.; Liu, J. Evaluation method of storage stability of SBS modified bitumen based on dynamic rheological properties. *Constr. Build. Mater.* **2022**, *323*, 126615. [CrossRef]
19. Akbari, A.; Akbari, A.; Ghanbari, A.; Hesami, S. Investigating the influence of aging and filler type on the fatigue behavior of bitumen mastics. *Constr. Build. Mater.* **2021**, *269*, 121254. [CrossRef]

20. Mahto, S.K.; Sinha, S. Application of marble dust and ground granulated blast-furnace slag in emulsified asphalt warm mixtures. *J. Clean. Prod.* **2022**, *370*, 133532. [CrossRef]
21. Marath, A.; Singh, D.; Rajan, B. Stiffness Behavior and Micromechanical Modeling of Asphalt Mastic Composed of Different Fillers. *J. Mater. Civ. Eng.* **2022**, *34*, 04022179. [CrossRef]
22. Zhao, X.; Ge, D.; Wang, J.; Wu, D.; Liu, J. The Performance Evaluation of Asphalt Mortar and Asphalt Mixture Containing Municipal Solid Waste Incineration Fly Ash. *Materials* **2022**, *15*, 1387. [CrossRef]
23. Russo, F.; Veropalumbo, R.; Oreto, C.; Cassese, D.; Papa, B.; Malvezzi, S. Reusing bottom ash as a filler from a Waste-to-Energy plant for making asphalt mastics. *Case Stud. Constr. Mater.* **2022**, *17*, e01406. [CrossRef]
24. Zhang, W.; Zou, L.; Wang, Y.; Liu, J.; Yang, C.; Di, J.; Hu, H.; Yang, Z. Influence of High Viscosity Petroleum Resin (HV-PR) on the Intermediate and High Temperature Performances of Styrene–Butadiene–Styrene Block Copolymer (SBS) Modified Bitumen. *Arab. J. Sci. Eng.* **2022**, *47*, 12521–12533. [CrossRef]
25. Mistry, R.; Roy, T.K. Performance evaluation of bituminous mix and mastic containing rice husk ash and fly ash as filler. *Constr. Build. Mater.* **2021**, *268*, 121187. [CrossRef]
26. Tiwari, N.; Satyam, N. Evaluation of Strength and Water Susceptibility Performance of Polypropylene Fiber–Reinforced and Silica Fume–Modified Hot Mix Asphalt. *Adv. Civ. Eng. Mater.* **2021**, *10*, 380–395. [CrossRef]
27. Choudhary, J.; Sukhija, M.; Gupta, A. A comparative analysis of engineering and economical suitability of bituminous mastics containing waste fillers. *Case Stud. Constr. Mater.* **2022**, *17*, e01640. [CrossRef]
28. Usman, K.R.; Hainin, M.R.; Satar, M.K.I.M.; Warid, M.N.M.; Kamarudin, S.N.N.; Abdulrahman, S. Palm oil fuel ash application in cold mix dense-graded bituminous mixture. *Constr. Build. Mater.* **2021**, *287*, 123033. [CrossRef]
29. Zhang, W.; Qiu, L.; Liu, J.; Hu, K.; Zou, L.; Chen, Y.; Yang, C.; Wang, F.; Zang, J. Modification mechanism of C9 petroleum resin and its influence on SBS modified asphalt. *Constr. Build. Mater.* **2021**, *306*, 124740. [CrossRef]
30. *JTG E42-2005*; Test Methods of Aggregate for Highway Engineering. China Communications Press: Beijing, China, 2005. (In Chinese)
31. *JTG E20-2011*; Standard Test Methods of Bitumen and Bituminous mixtures for Highway Engineering. China Communications Press: Beijing, China, 2011. (In Chinese)
32. Yao, Z.; Yang, R.; Liu, Z.; An, H.; Zhang, Q.; Yuan, W. Study on the Applicability of Needle/Cone Penetration Experiment for Asphalt-Rubber. *Adv. Civ. Eng.* **2020**, *2020*, 8328412. [CrossRef]
33. Yang, S.; Jiang, J.; Leng, Z.; Ni, F. Feasibility and performance of the Semi-circular Bending test in evaluating the low-temperature performance of asphalt mortar. *Constr. Build. Mater.* **2021**, *269*, 121305. [CrossRef]
34. Xiao, F.; Li, R.; Zhang, H.; Amirkhanian, S. Low Temperature Performance Characteristics of Reclaimed Asphalt Pavement (RAP) Mortars with Virgin and Aged Soft Binders. *Appl. Sci.* **2017**, *7*, 304. [CrossRef]
35. Moon, K.H.; Falchetto, A.C.; Wang, D.; Riccardi, C.; Wistuba, M.P. Mechanical Performance of Asphalt Mortar Containing Hydrated Lime and EAFSS at Low and High Temperatures. *Materials* **2017**, *10*, 743. [CrossRef] [PubMed]
36. *JTG F40-2004*; Technical Specification of Construction of Highway Asphalt Pavement. China Communications Press: Beijing, China, 2004. (In Chinese)
37. Niu, T.; Roque, R.; Lopp, G.A. Development of a binder fracture test to determine fracture energy properties. *Road Mater. Pavement Des.* **2014**, *15*, 219–238. [CrossRef]

Disclaimer/Publisher's Note: The statements, opinions and data contained in all publications are solely those of the individual author(s) and contributor(s) and not of MDPI and/or the editor(s). MDPI and/or the editor(s) disclaim responsibility for any injury to people or property resulting from any ideas, methods, instructions or products referred to in the content.